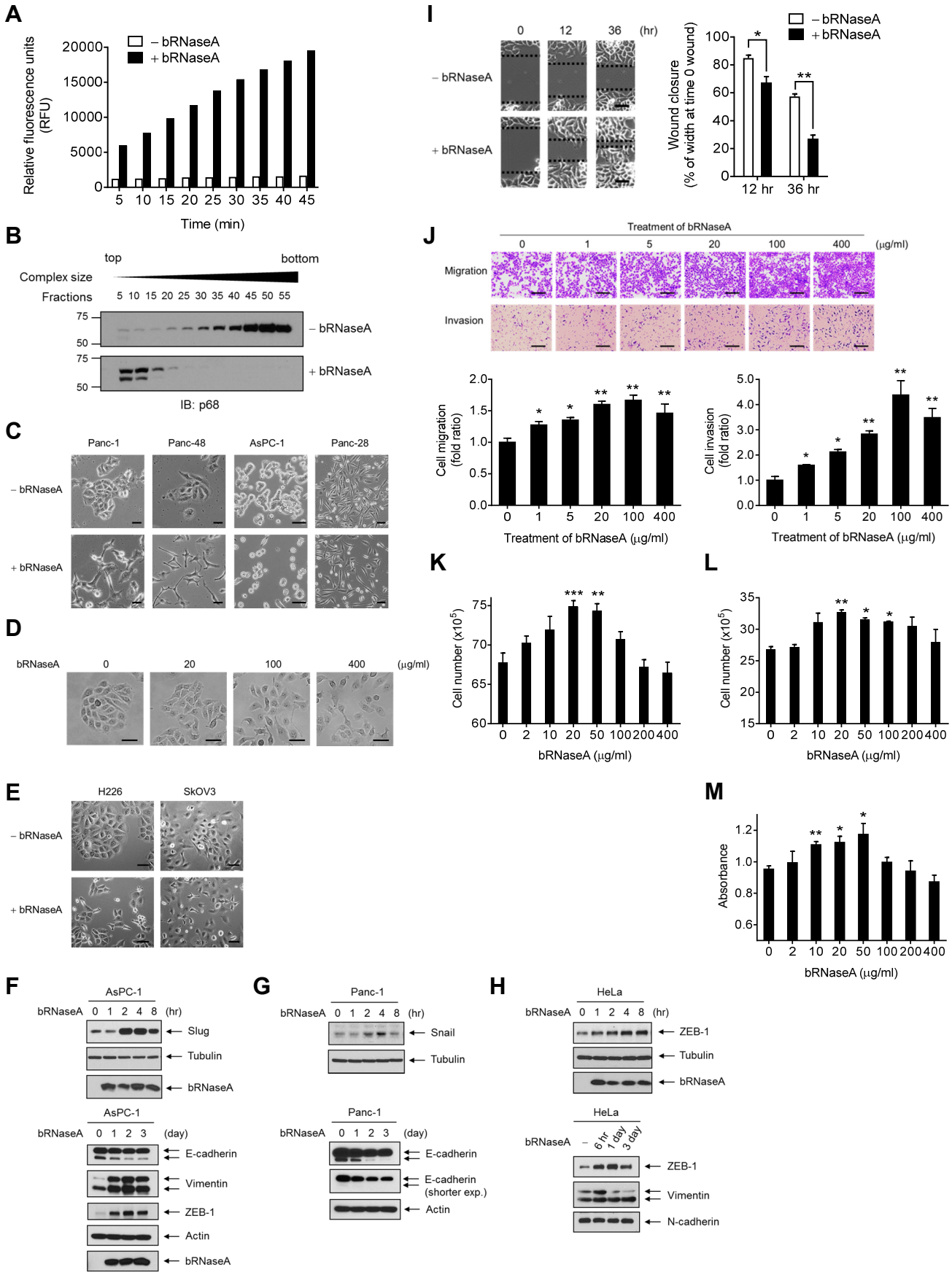
A
Relative fluorescence units (RFU)
20000
15000
10000
5000
0
– bRNaseA
+ bRNaseA
5 10 15 20 25 30 35 40 45
Time (min)
B
top
bottom
Complex size
Fractions
5 10 15 20 25 30 35 40 45 50 55
75
50
– bRNaseA
+ bRNaseA
IB: p68
C
Panc-1
Panc-48
AsPC-1
Panc-28
– bRNaseA
+ bRNaseA
D
bRNaseA
0
20
100
400
(μg/ml)
E
H226
SkOV3
– bRNaseA
+ bRNaseA
F
AsPC-1
bRNaseA 0 1 2 4 8 (hr)
Slug
Tubulin
bRNaseA
AsPC-1
bRNaseA 0 1 2 3 (day)
E-cadherin
Vimentin
ZEB-1
Actin
bRNaseA
G
Panc-1
bRNaseA 0 1 2 4 8 (hr)
Snail
Tubulin
Panc-1
bRNaseA 0 1 2 3 (day)
E-cadherin
E-cadherin (shorter exp.)
Actin
H
HeLa
bRNaseA 0 1 2 4 8 (hr)
ZEB-1
Tubulin
bRNaseA
HeLa
bRNaseA – 6 hr 1 day 3 day
ZEB-1
Vimentin
N-cadherin
I
0
12
36
(hr)
– bRNaseA
+ bRNaseA
Wound closure (% of width at time 0 wound)
100
80
60
40
20
0
– bRNaseA
+ bRNaseA
*
**
12 hr
36 hr
J
Treatment of bRNaseA
0
1
5
20
100
400
(μg/ml)
Migration
Invasion
Cell migration (fold ratio)
2.0
1.5
1.0
0.5
0.0
0 1 5 20 100 400
Treatment of bRNaseA (μg/ml)
Cell invasion (fold ratio)
5.0
4.0
3.0
2.0
1.0
0.0
0 1 5 20 100 400
Treatment of bRNaseA (μg/ml)
K
Cell number (x10^5)
75
70
65
60
0 2 10 20 50 100 200 400
bRNaseA (μg/ml)
L
Cell number (x10^5)
35
30
25
20
15
0 2 10 20 50 100 200 400
bRNaseA (μg/ml)
M
Absorbance
1.2
1.0
0.8
0.6
0 2 10 20 50 100 200 400
bRNaseA (μg/ml)

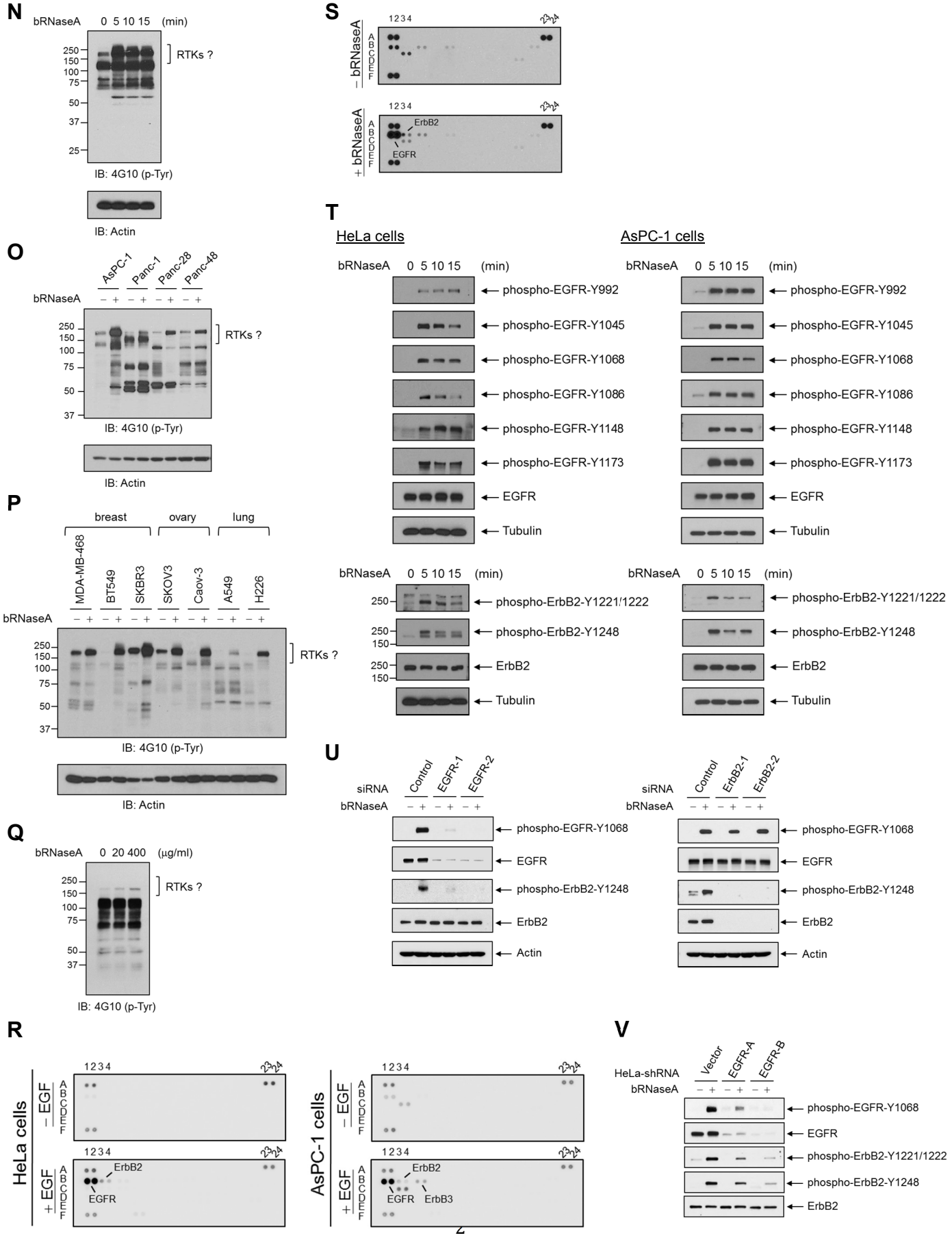
N
bRNaseA 0 5 10 15 (min)
250
150
100
75
50
37
25
RTKs ?
IB: 4G10 (p-Tyr)
IB: Actin
O
AsPC-1
Panc-1
Panc-28
Panc-48
bRNaseA
– + – + – + – +
250
150
100
75
50
37
RTKs ?
IB: 4G10 (p-Tyr)
IB: Actin
P
breast
ovary
lung
MDA-MB-468
BT549
SKBR3
SKOV3
Caov-3
A549
H226
bRNaseA
– + – + – + – + – + – + – +
250
150
100
75
50
37
RTKs ?
IB: 4G10 (p-Tyr)
IB: Actin
Q
bRNaseA 0 20 400 (μg/ml)
250
150
100
75
50
37
RTKs ?
IB: 4G10 (p-Tyr)
R
HeLa cells
– EGF
+ EGF
A B C D E F
1 2 3 4
23 24
ErbB2
EGFR
AsPC-1 cells
– EGF
+ EGF
A B C D E F
1 2 3 4
23 24
ErbB2
EGFR
ErbB3
S
– bRNaseA
+ bRNaseA
A B C D E F
1 2 3 4
23 24
ErbB2
EGFR
T
HeLa cells
AsPC-1 cells
bRNaseA 0 5 10 15 (min)
phospho-EGFR-Y992
phospho-EGFR-Y1045
phospho-EGFR-Y1068
phospho-EGFR-Y1086
phospho-EGFR-Y1148
phospho-EGFR-Y1173
EGFR
Tubulin
bRNaseA 0 5 10 15 (min)
250
250
150
250
150
phospho-ErbB2-Y1221/1222
phospho-ErbB2-Y1248
ErbB2
Tubulin
U
siRNA Control EGFR-1 EGFR-2
bRNaseA – + – + – +
phospho-EGFR-Y1068
EGFR
phospho-ErbB2-Y1248
ErbB2
Actin
siRNA Control ErbB2-1 ErbB2-2
bRNaseA – + – + – +
phospho-EGFR-Y1068
EGFR
phospho-ErbB2-Y1248
ErbB2
Actin
V
HeLa-shRNA Vector EGFR-A EGFR-B
bRNaseA – + – + – +
phospho-EGFR-Y1068
EGFR
phospho-ErbB2-Y1221/1222
phospho-ErbB2-Y1248
ErbB2

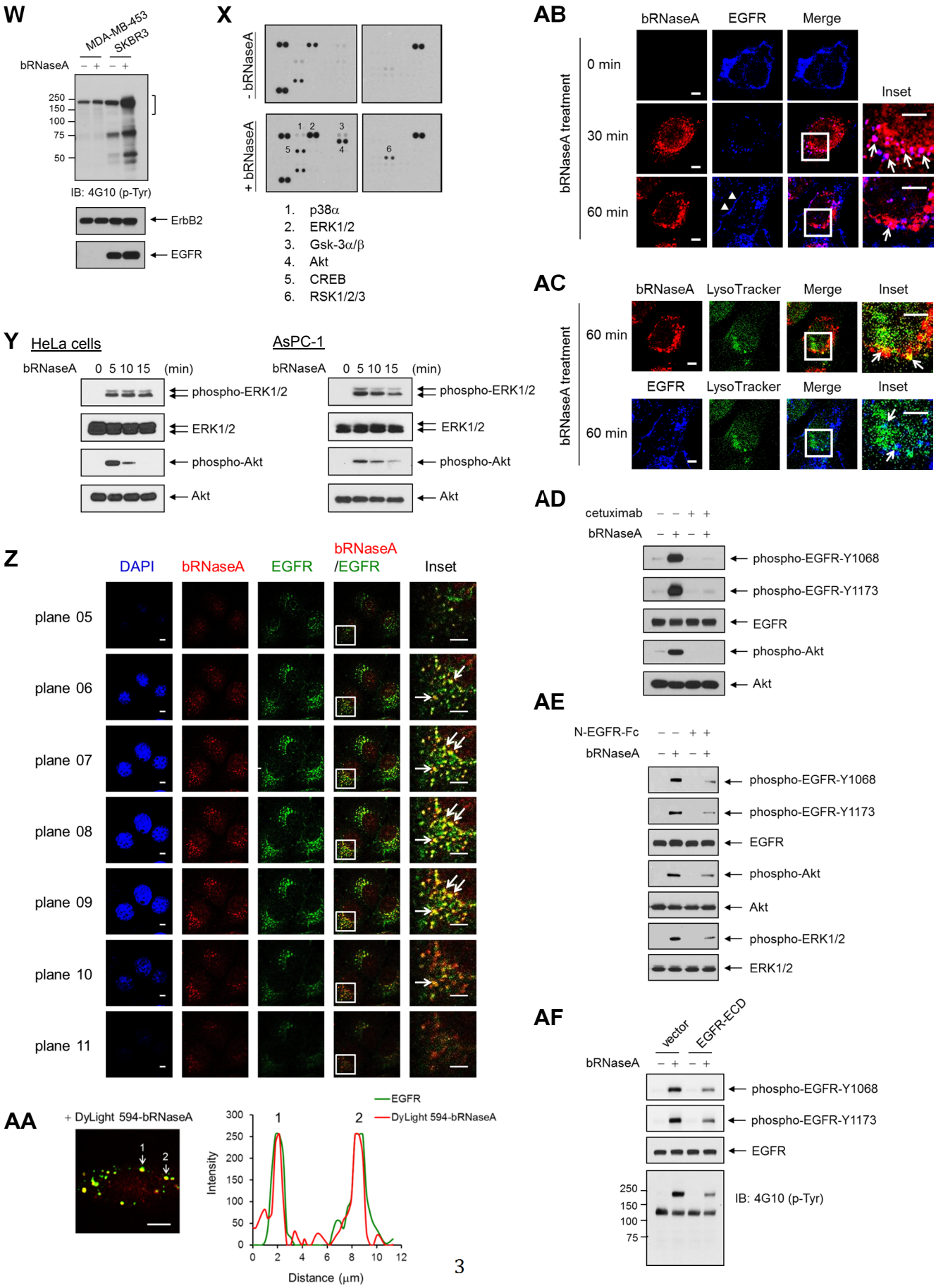
W
MDA-MB-453
SKBR3
bRNaseA
250
150
100
75
50
IB: 4G10 (p-Tyr)
ErbB2
EGFR
X
- bRNaseA
+ bRNaseA
1. p38α
2. ERK1/2
3. Gsk-3α/β
4. Akt
5. CREB
6. RSK1/2/3
AB
bRNaseA
EGFR
Merge
Inset
bRNaseA treatment
0 min
30 min
60 min
AC
bRNaseA
LysoTracker
Merge
Inset
EGFR
60 min
Y
HeLa cells
AsPC-1
bRNaseA 0 5 10 15 (min)
phospho-ERK1/2
ERK1/2
phospho-Akt
Akt
AD
cetuximab
bRNaseA
phospho-EGFR-Y1068
phospho-EGFR-Y1173
EGFR
phospho-Akt
Akt
Z
DAPI
bRNaseA
EGFR
bRNaseA /EGFR
Inset
plane 05
plane 06
plane 07
plane 08
plane 09
plane 10
plane 11
AE
N-EGFR-Fc
bRNaseA
phospho-EGFR-Y1068
phospho-EGFR-Y1173
EGFR
phospho-Akt
Akt
phospho-ERK1/2
ERK1/2
AA
+ DyLight 594-bRNaseA
EGFR
DyLight 594-bRNaseA
Intensity
Distance (μm)
AF
vector
EGFR-ECD
bRNaseA
phospho-EGFR-Y1068
phospho-EGFR-Y1173
EGFR
IB: 4G10 (p-Tyr)

AG

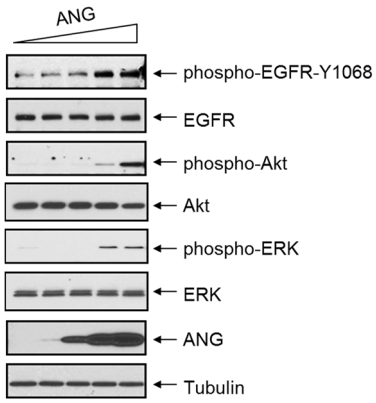

AH

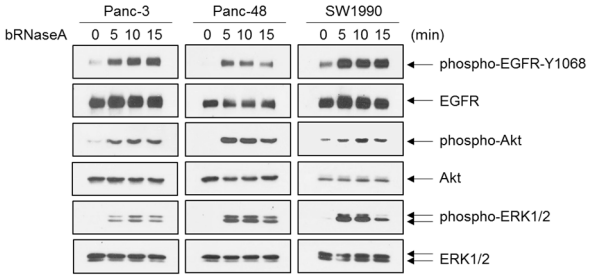

AI

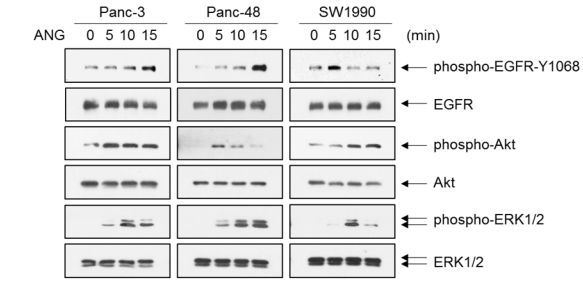

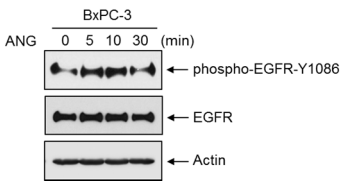

AJ

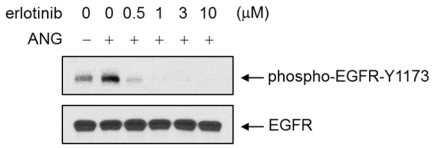

AK

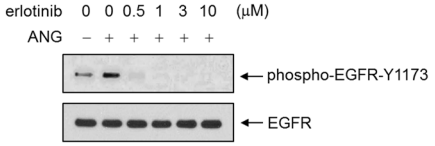

AL

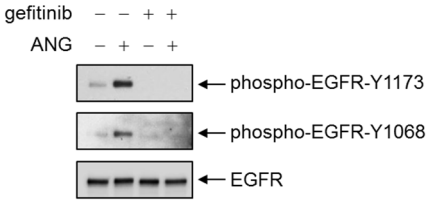

AM

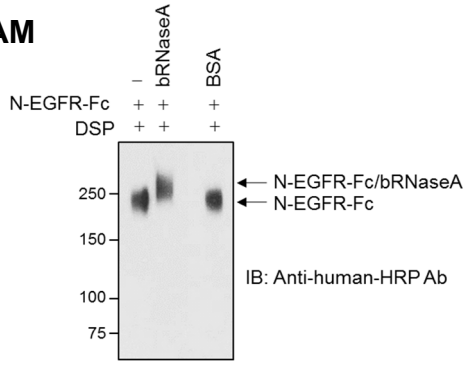

AN

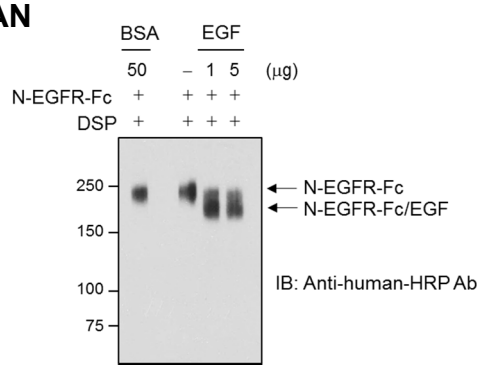

AO

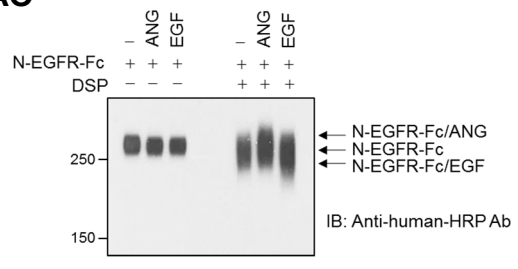

Figure S1. bRNaseA and ANG associate with EGFR and induce EGFR signaling cascades. Related to Figure 1.

(A) Detection of bRNaseA enzyme activity, at 50 pg/ml, using an RNaseAlert® Lab Test kit monitored by a real-time fluorometer.

(B) Sedimentation pattern of p68 RNA helicase, a RNA binding protein as a positive control, through linear 10-40% (top-bottom) sucrose gradients.

(C) Images showing morphological changes in pancreatic cells treated with bRNaseA (100 μg/ml) for 2 days. Bar, 100 μm.

(D) Images showing morphological changes in HeLa cells treated with bRNaseA at the indicated concentrations for 1 day. Bar, 100 μm.

(E) Images showing morphological changes in H226 (lung) and SkOV3 (ovarian) cancer cells treated with bRNaseA (100 μg/ml) for 2 days. Bar, 100 μm.

(F–H) IB of AsPC-1 (F), Panc-1 (G), and HeLa (H) cells treated with bRNaseA (100 μg/ml) at various time points and probed with the indicated EMT antibodies.

(I) Wound healing assay of HeLa cells treated with bRNaseA (100 μg/ml) at the indicated time points. Bar, 200 μm. The distance of the wound gaps was determined by using the ImageJ software program (version 1.38x; National Institutes of Health) and normalized against the width at time 0, which was plotted diagrammatically in the right panel. Error bars represent SD. *$p < 0.05$; **$p < 0.01$, Student's *t*-test.

(J) Top, representative images of migration (in transwells) and invasion (in matrigel-coated invasion chambers) of HeLa cells treated with bRNaseA at various concentrations for 3 days. Bar, 500 μm. Bottom, quantification of cell migration and invasion. Error bars represent SD. *$p < 0.05$; **$p < 0.01$, Student's *t*-test.

(K and L) Cell counting, measured by a Coulter® Particle Counter (Beckman Coulter) of MDBK (K) and HeLa (L) cells treated with bRNaseA at various concentrations for 3 days. Error bars represent SD. *p < 0.05; **p < 0.01; ***p < 0.001, Student's *t*-test.

(M) Cell viability assay of HeLa cells treated with various concentrations of bRNaseA. Absorbance was measured at 595 nm with a reference wavelength of 650 nm.

(N) IB of HeLa cells treated with bRNaseA (100 μg/ml) at the indicated time points and probed with a phospho-tyrosine (p-Tyr) antibody.

(O–Q) IB of pancreatic (O), breast, ovarian, and lung cancer cells (P), and bovine MDBK cells (Q), treated with bRNaseA (100 μg/ml or the indicated concentrations) for 5 min and probed with a p-Tyr antibody.

(R) Human phospho-RTK antibody array analysis of HeLa (left) and AsPC-1 (right) cells treated with or without EGF (50 ng/ml) for 5 min.

(S) Human phospho-RTK antibody array analysis of AsPC-1 cells treated with or without bRNaseA (100 μg/ml) for 5 min.

(T) IB of HeLa (left) and AsPC-1 (right) cells treated with bRNaseA (100 μg/ml) at various time points.

(U and V) IB of HeLa cells transfected with individual small interfering RNAs (siRNAs) against EGFR and ErbB2 (U) and EGFR-deficient HeLa stable transfectants expressing small hairpin RNA (shRNA) targeting EGFR (V) in the presence or absence of bRNaseA (100 μg/ml).

(W) IB of MDA-MB-453 and SKBR3 cells treated with or without bRNaseA (100 μg/ml).

(X) Human phospho-kinase antibody array analysis of AsPC-1 cells treated with or without bRNaseA (100 μg/ml) for 5 min.

(Y) IB of HeLa (left) and AsPC-1 (right) cells treated with bRNaseA (100 μg/ml) at different

time points.

(Z) Confocal microscopy of HeLa cells stained with DAPI (blue), bRNaseA (red), or EGFR (green) antibodies. A single cell was dissected into 32 focal sections with a thickness of 0.5 μm each. The nucleus spanned between focal plans 04-12. Co-localization of EGFR and bRNaseA, as indicated by the yellow signals in the merged images, is shown from plans 06-10 in the insets (white arrows). Insets, enlargements of the boxed areas (10.0× magnification). Bar, 5 μm.

(AA) Intensity profile of two yellow signals (arrows in the merged image) as shown in inset 1 in Figure 1H. Bar, 5 μm.

(AB) Confocal microscopy of HeLa cells stained with bRNaseA (red) and EGFR (blue) antibodies. Insets, enlargements of the boxed areas (7.0× magnification). Bar, 5 μm.

(AC) Confocal microscopy of HeLa cells stained with LysoTracker (green) and bRNaseA (red) or EGFR (blue) antibodies. Insets, enlargements of the boxed areas (7.0× magnification). Bar, 5 μm.

(AD) IB of HeLa cells pretreated with cetuximab (10 μg/ml) at 4 °C for 1 hr and followed by bRNaseA stimulation (100 μg/ml).

(AE) IB of HeLa cells pre-incubated with or without N-EGFR-Fc in the presence or absence of bRNaseA (100 μg/ml).

(AF) IB of HeLa cells transfected with empty vector and the extracellular domain of EGFR (EGFR-ECD) in the presence or absence of bRNaseA (100 μg/ml).

(AG) IB of HeLa cells treated with increasing concentrations (0.2, 0.5, 1, 2 μg/ml) of ANG for 5 min.

(AH and AI) IB of pancreatic cancer cells treated with bRNaseA (100 μg/ml) (AH) or ANG (1 μg/ml) (AI) at the indicated time points.

(AJ and AK) IB of AsPC-1 (AJ) and Panc-1 (AK) cells pretreated with erlotinib (10 μM), followed by ANG (1 μg/ml) treatment for 5 min.

(AL) IB of HeLa cells pretreated with gefitinib (10 μM), followed by ANG (1 μg/ml) treatment for 5 min.

(AM and AN) In vitro binding assay of N-EGFR-Fc with bRNaseA (AM) or EGF (AN) cross-linked with [dithiobis(succinimidylpropionate)] (DSP) followed by IB under a non-reducing and non-denaturing condition. BSA serves as a negative control.

(AO) In vitro binding assay of N-EGFR-Fc with ANG or EGF cross-linked with or without DSP followed by IB under a non-reducing and non-denaturing condition.

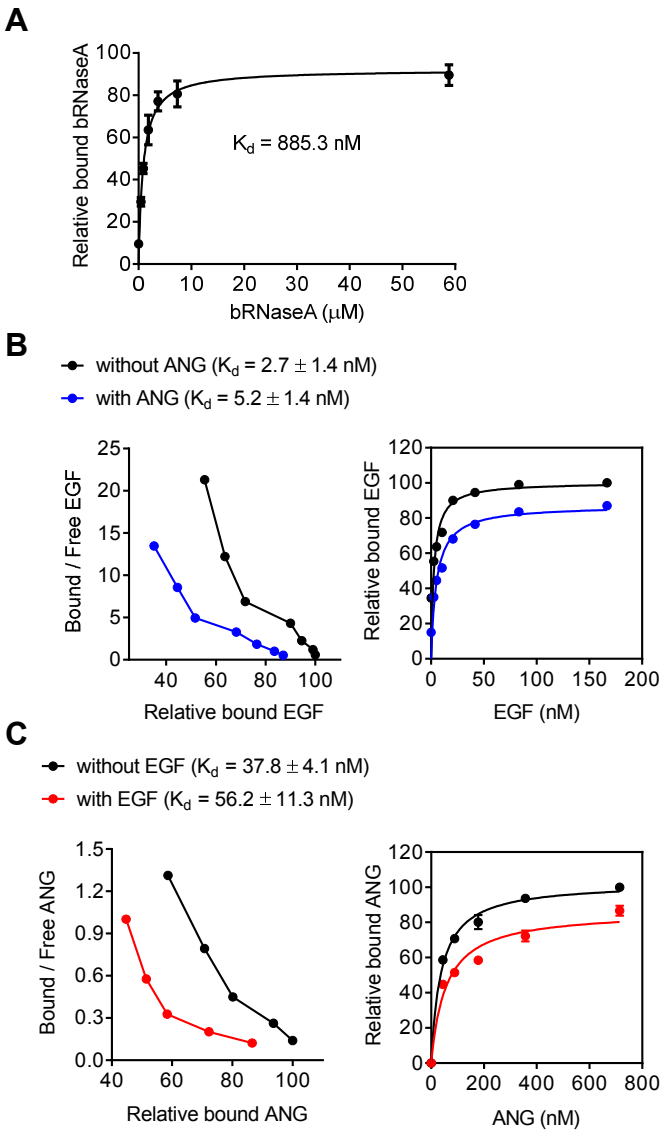

Figure S2. ANG competes with EGF for EGFR binding. Related to Figure 2.

(A) Saturation binding assay of the K_d value determination for bRNaseA binding toward EGFR in A431 cell lysates.

(B) Scatchard plot (left) and binding curves (right), which measured EGFR-EGF binding affinity of A431 cells with or without ANG (5 μg/ml equivalent to 357.14 nM) treatment.

(C) Scatchard plot (left) and binding curves (right), which measured EGFR-ANG binding affinity of A431 cells with or without EGF (300 ng/ml equivalent to 50 nM) treatment.

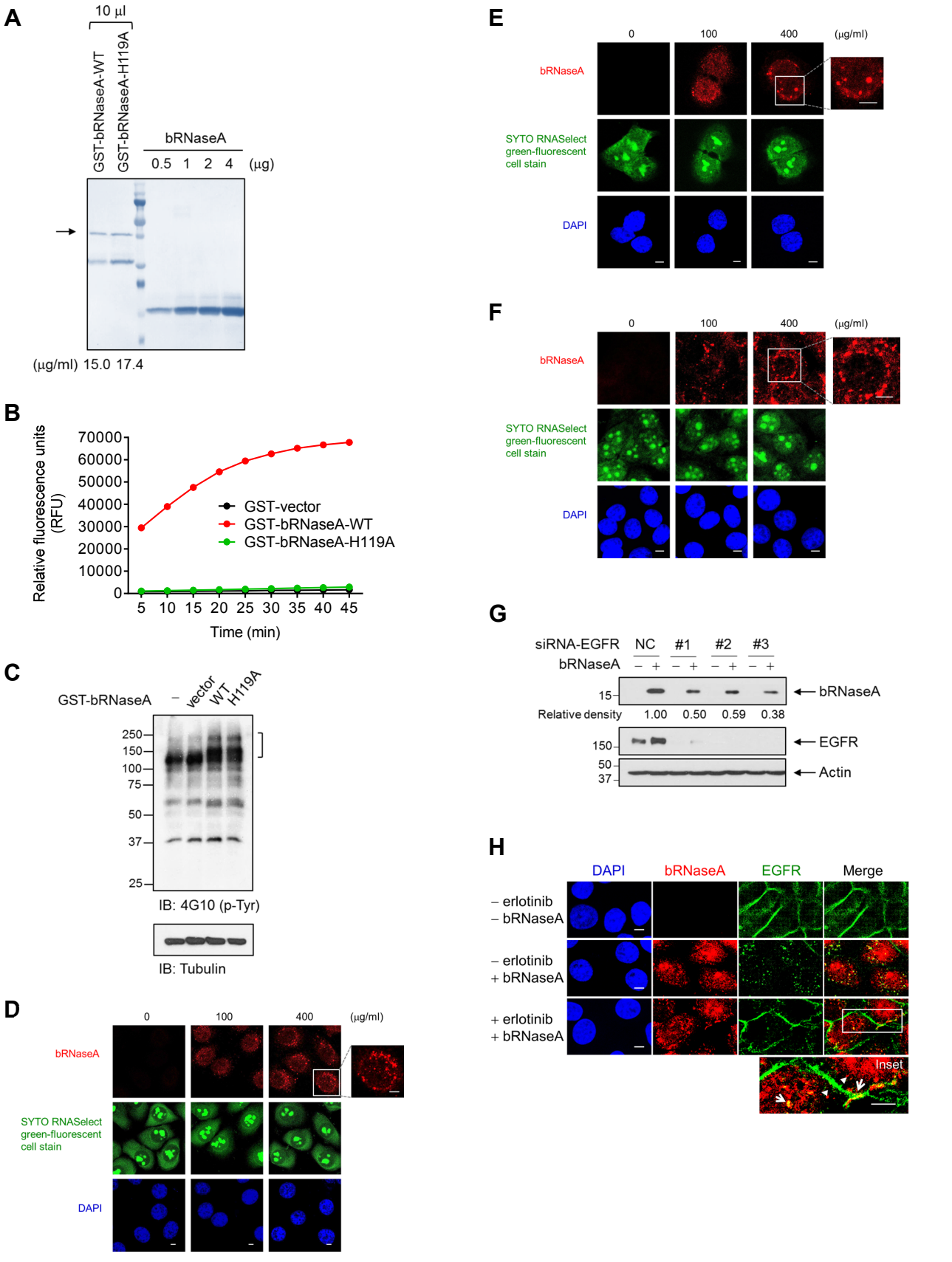
A
10 µl
GST-bRNaseA-WT
GST-bRNaseA-H119A
bRNaseA
0.5 1 2 4 (µg)
(µg/ml) 15.0 17.4
B
Relative fluorescence units (RFU)
70000
60000
50000
40000
30000
20000
10000
0
5 10 15 20 25 30 35 40 45
Time (min)
GST-vector
GST-bRNaseA-WT
GST-bRNaseA-H119A
C
GST-bRNaseA – vector WT H119A
250
150
100
75
50
37
25
IB: 4G10 (p-Tyr)
IB: Tubulin
D
0 100 400 (µg/ml)
bRNaseA
SYTO RNASelect green-fluorescent cell stain
DAPI
E
0 100 400 (µg/ml)
bRNaseA
SYTO RNASelect green-fluorescent cell stain
DAPI
F
0 100 400 (µg/ml)
bRNaseA
SYTO RNASelect green-fluorescent cell stain
DAPI
G
siRNA-EGFR NC #1 #2 #3
bRNaseA – + – + – + – +
15
bRNaseA
Relative density 1.00 0.50 0.59 0.38
150
EGFR
50
37
Actin
H
DAPI bRNaseA EGFR Merge
– erlotinib
– bRNaseA
– erlotinib
+ bRNaseA
+ erlotinib
+ bRNaseA
Inset

Figure S3. Catalytic activity of RNase is not required for activation of and binding to EGFR. Related to Figure 3.

(A) Coomassie blue staining of GST-tagged plasmids and increasing amounts of recombinant bRNaseA.

(B) Detection of RNase enzyme activity of the indicated plasmids with use of an RNaseAlert® Lab Test kit monitored by a real-time fluorimeter.

(C) IB of HeLa cells treated with the indicated proteins or water (–) for 5 min.

(D–F) Confocal microscopy of HeLa (D), AsPC-1 (E), and MDBK (F) cells, treated with the indicated concentrations of bRNaseA for 30 min and stained with DAPI (blue), bRNaseA antibody (red), or SYTO® RNASelect™ green-fluorescent cell stain (green). Insets, enlargements of the boxed areas (4.0× magnification). Bar, 5 μm.

(G) IB of HeLa cells transfected with individual siRNAs against EGFR in the presence or absence of bRNaseA for 30 min.

(H) Confocal microscopy of HeLa cells pretreated with erlotinib at 37 °C for 18 hr followed by bRNaseA treatment for 30 min and staining with DAPI (blue), bRNaseA (red), or EGFR antibodies (green). Inset, enlargements of the boxed area (6.0× magnification). Bar, 10 μm

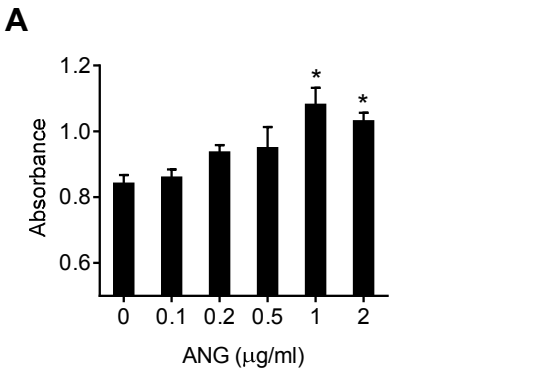

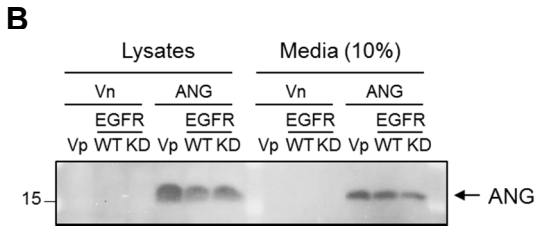

C

		Tissue ANG		
		Low	High	Total
Plasma ANG	Low	6	1	7
	High	1	6	7
Total		7	7	14

p = 0.03

Figure S4. A positive correlation between ANG levels in tumor tissues and their matched plasma in pancreatic cancer patients. Related to Figure 4.

(A) Cell viability assay of HeLa cells treated the indicated concentrations of ANG. Absorbance was measured at 595 nm with a reference wavelength of 650 nm. Error bars represent SD. *$p < 0.05$, Student's *t*-test.

(B) IB of lysates and 10% of the secreted proteins from CM in NIH-3T3 stable transfectants expressing the indicated plasmids.

(C) Quantification for the correlation between tissue ANG and plasma ANG in pancreatic cancer patients. Fisher's exact test.

Table S1. Determination of ANG, hRNase1, EGF, and TGF-α proteins in the plasma of pancreatic cancer patients. Related to Figure 5.

Experiment-1					
		Normal		**Cancer**	
variables	**n**	**Median (range; pg/ml)**	**n**	**Median (range; pg/ml)**	**p value**
ANG	10	341053.95 (273450.31-765434.13)	30	458840.09 (273903.31-996966.31)	0.014
hRNase1	10	928456.06 (614538.13-1767189.9)	30	945943.16 (629581.25-1542261.1)	0.827
EGF	9	17.65 (1.87-58.860001)	28	18.07 (.31999999-120.06)	0.860
TGF-α	10	14.994 (12.959-24.878)	30	15.576 (12.378-44.355)	0.851
Experiment-2					
		Normal		**Cancer**	
variables	**n**	**Median (range; pg/ml)**	**n**	**Median (range; pg/ml)**	**p value**
ANG	20	220767.89 (43273-478269)	20	327361.2 (125984-569699)	0.011
hRNase1	11	1017414.63 (1674331-526226)	19	1278614.53 (2662773-462952)	0.45

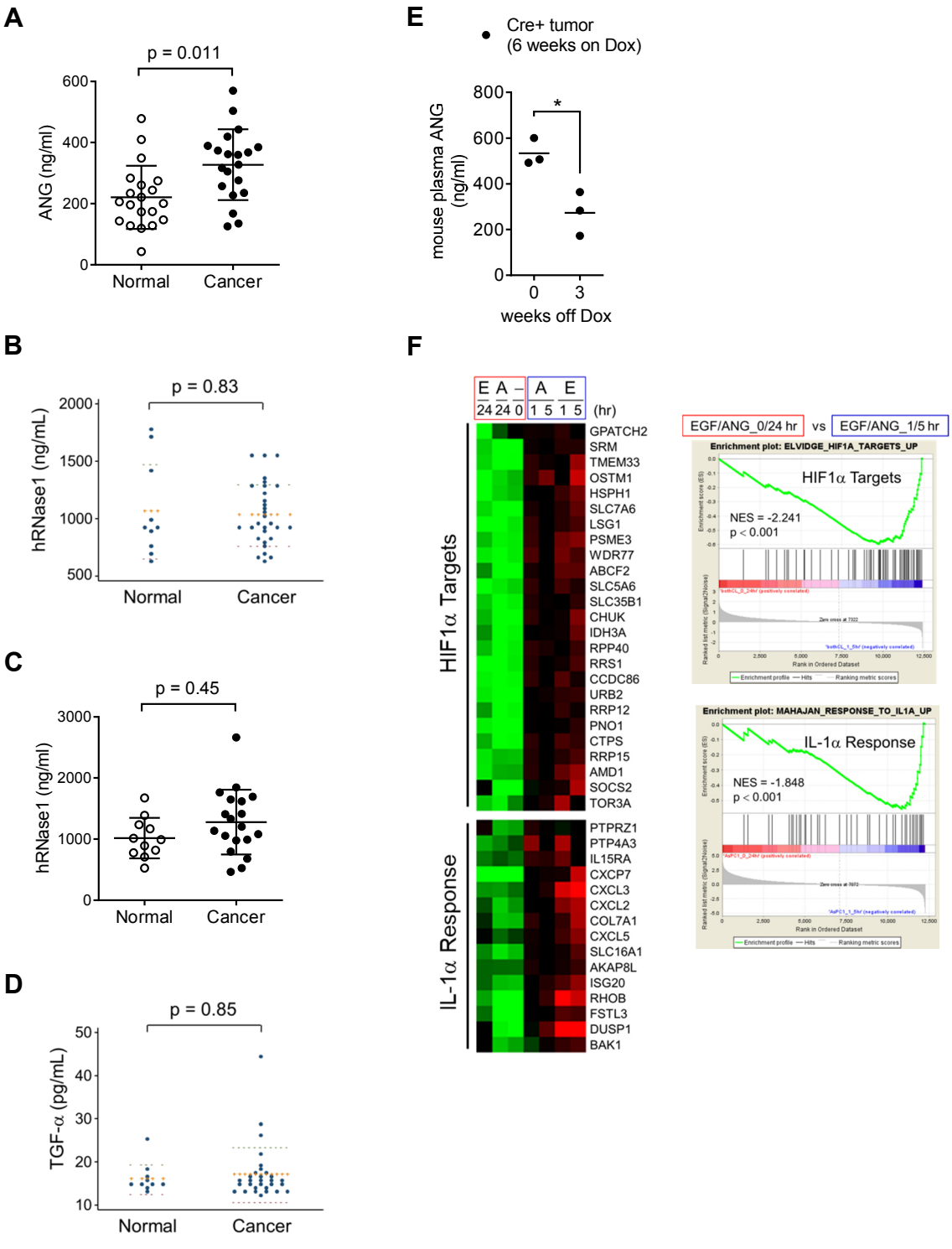
A
p = 0.011
ANG (ng/ml)
600
400
200
0
Normal
Cancer
B
p = 0.83
hRNase1 (ng/mL)
2000
1500
1000
500
Normal
Cancer
C
p = 0.45
hRNase1 (ng/ml)
3000
2000
1000
0
Normal
Cancer
D
p = 0.85
TGF-α (pg/mL)
50
40
30
20
10
Normal
Cancer
E
Cre+ tumor
(6 weeks on Dox)
mouse plasma ANG (ng/ml)
800
600
400
200
0
*
0
3
weeks off Dox
F
E A – A E
24 24 0 1 5 1 5 (hr)
HIF1α Targets
GPATCH2
SRM
TMEM33
OSTM1
HSPH1
SLC7A6
LSG1
PSME3
WDR77
ABCF2
SLC5A6
SLC35B1
CHUK
IDH3A
RPP40
RRS1
CCDC86
URB2
RRP12
PNO1
CTPS
RRP15
AMD1
SOCS2
TOR3A
IL-1α Response
PTPRZ1
PTP4A3
IL15RA
CXCP7
CXCL3
CXCL2
COL7A1
CXCL5
SLC16A1
AKAP8L
ISG20
RHOB
FSTL3
DUSP1
BAK1
EGF/ANG_0/24 hr
vs
EGF/ANG_1/5 hr
Enrichment plot: ELVIDGE_HIF1A_TARGETS_UP
HIF1α Targets
NES = -2.241
p < 0.001
Enrichment plot: MAHAJAN_RESPONSE_TO_IL1A_UP
IL-1α Response
NES = -1.848
p < 0.001

Figure S5. No significant differences in levels of hRNase1 and traditional EGFR ligands between the normal and pancreatic cancer patient samples. Related to Figure 5.

(A–D) ELISA assay of ANG (A; Experiment-2), hRNase1 (B; Experiment-1 and C; Experiment-2), and TGF-α (D; Experiment-1) in plasma samples of pancreatic cancer patients for comparison with a noncancerous normal group.

(E) ELISA of ANG level in plasma samples of *iKras;p53*$^{L/+}$ PDAC mice (Cre^{+} tumor), followed by Dox withdrawal for 3 weeks. Line indicates the mean. *$p < 0.05$, Student's *t*-test.

(F) Left, heat maps of the genes expressed in HIF1α targets and IL-1α response upon EGF (50 ng/ml) and ANG (1 μg/ml) treatment in the indicated time points in AsPC-1 cells. Right, representative GSEA results showing activated signaling pathways in both EGF (50 ng/ml) and ANG (1 μg/ml) treatment (1/5-hr cluster versus 0/24-hr cluster). NES, normalized enrichment score.

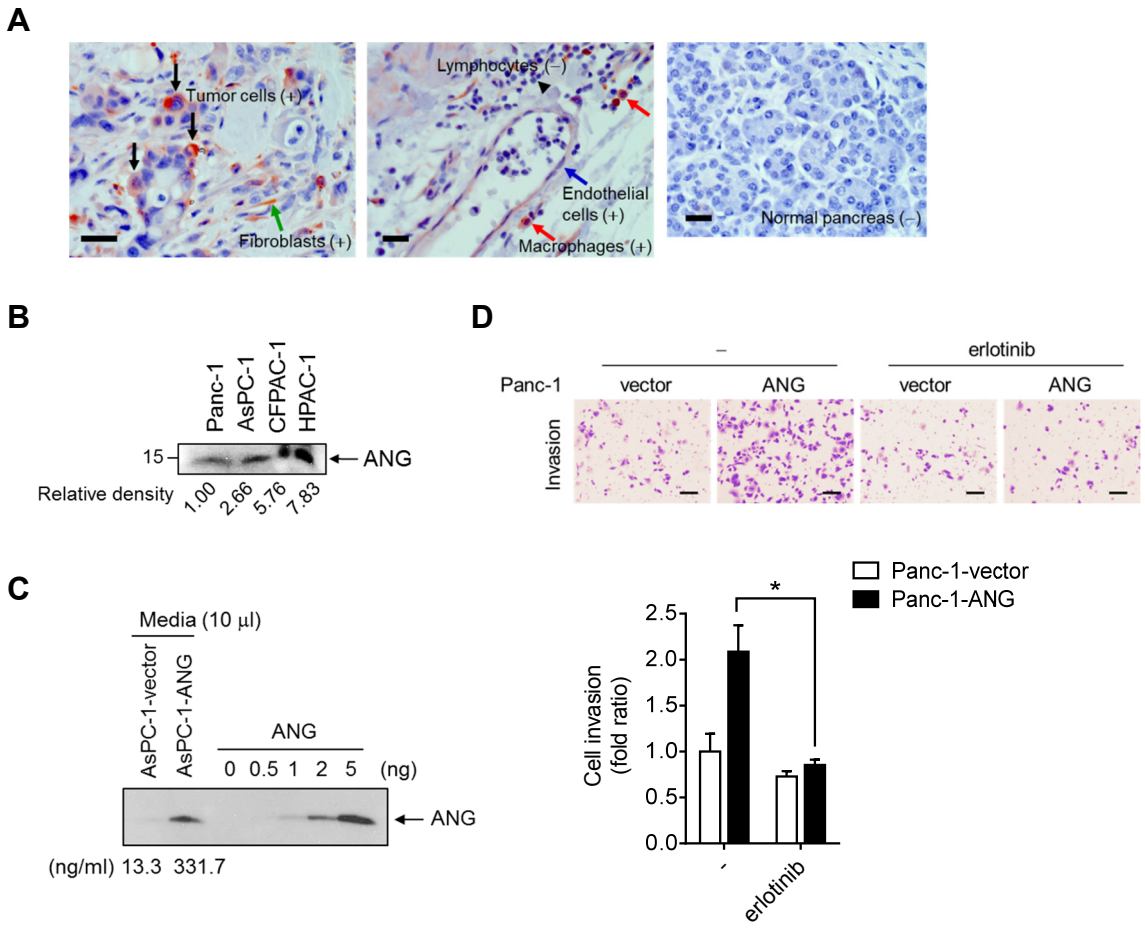

Figure S6. EGFR activation is responsible for ANG-triggered cell invasion in Panc-1 cells. Related to Figure 6.

(A) Immunohistochemistry staining of representative cases in human pancreatic tumor tissues stained with anti-ANG antibody. Positive (+) signals: tumor cells (black arrows), fibroblasts (green arrow), macrophages (red arrows), and endothelial cells (blue arrow); negative (–) signals: lymphocytes (arrowhead) and normal pancreas. Bar, 50 µm.

(B) Analysis of the expression level of ANG protein secreted in pancreatic cancer cell media by normalizing the cell number to 30,000 for each cell line.

(C) IB of secreted proteins in AsPC-1 stable transfectants expressing ANG (AsPC-1-ANG) and empty vector (AsPC-1-vector), compared with increasing amounts of recombinant ANG proteins. (D) Top, representative images of cell invasion assay of Panc-1 stable transfectants expressing empty vector and ANG treated with or without erlotinib. Bar, 200 μm. Bottom, quantification of cell invasion. Error bars represent SD. *$p < 0.05$, Student's *t*-test.

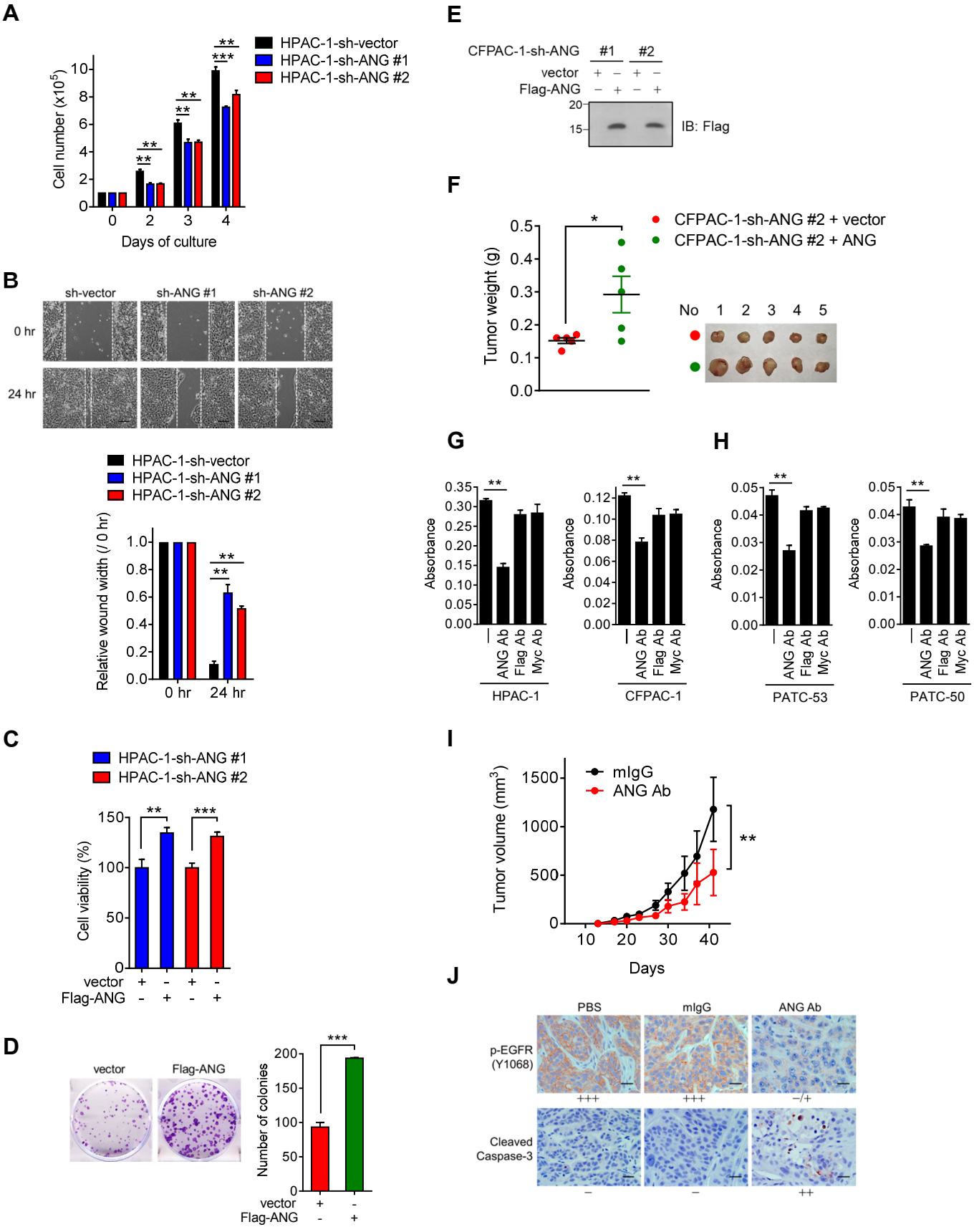
A
HPAC-1-sh-vector
HPAC-1-sh-ANG #1
HPAC-1-sh-ANG #2
Cell number (x10^5)
Days of culture
B
sh-vector
sh-ANG #1
sh-ANG #2
0 hr
24 hr
HPAC-1-sh-vector
HPAC-1-sh-ANG #1
HPAC-1-sh-ANG #2
Relative wound width (/ 0 hr)
0 hr
24 hr
C
HPAC-1-sh-ANG #1
HPAC-1-sh-ANG #2
Cell viability (%)
vector
Flag-ANG
D
vector
Flag-ANG
Number of colonies
vector
Flag-ANG
E
CFPAC-1-sh-ANG
#1
#2
vector
Flag-ANG
IB: Flag
F
CFPAC-1-sh-ANG #2 + vector
CFPAC-1-sh-ANG #2 + ANG
Tumor weight (g)
No 1 2 3 4 5
G
Absorbance
— ANG Ab Flag Ab Myc Ab
HPAC-1
CFPAC-1
H
Absorbance
— ANG Ab Flag Ab Myc Ab
PATC-53
PATC-50
I
mIgG
ANG Ab
Tumor volume (mm^3)
Days
J
PBS
mIgG
ANG Ab
p-EGFR (Y1068)
+++
+++
–/+
Cleaved Caspase-3
–
–
++

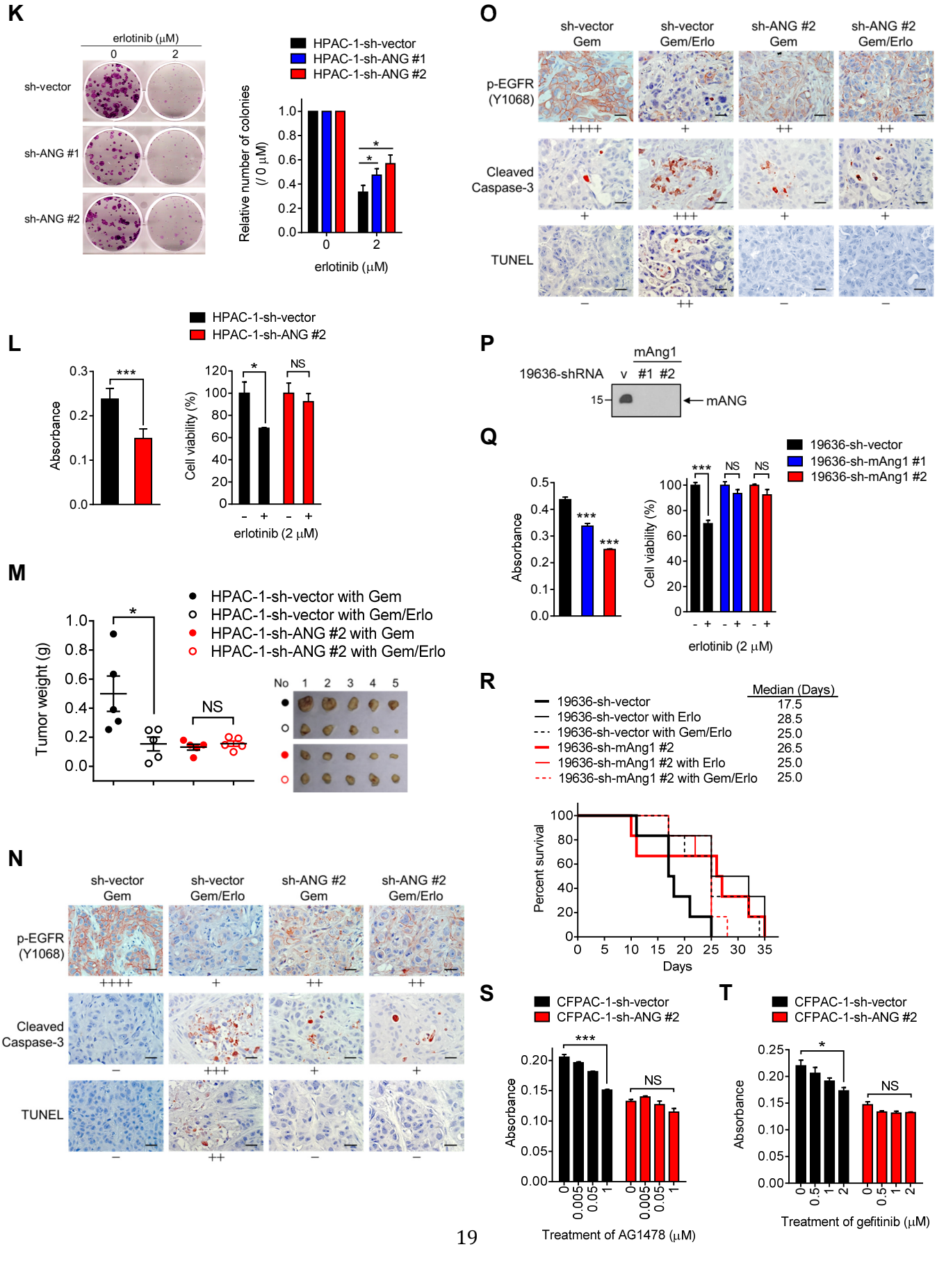
K
erlotinib (μM)
0
2
sh-vector
sh-ANG #1
sh-ANG #2
HPAC-1-sh-vector
HPAC-1-sh-ANG #1
HPAC-1-sh-ANG #2
Relative number of colonies (/ 0 μM)
erlotinib (μM)
L
HPAC-1-sh-vector
HPAC-1-sh-ANG #2
Absorbance
Cell viability (%)
NS
erlotinib (2 μM)
M
HPAC-1-sh-vector with Gem
HPAC-1-sh-vector with Gem/Erlo
HPAC-1-sh-ANG #2 with Gem
HPAC-1-sh-ANG #2 with Gem/Erlo
Tumor weight (g)
NS
No 1 2 3 4 5
N
sh-vector Gem
sh-vector Gem/Erlo
sh-ANG #2 Gem
sh-ANG #2 Gem/Erlo
p-EGFR (Y1068)
Cleaved Caspase-3
TUNEL
O
sh-vector Gem
sh-vector Gem/Erlo
sh-ANG #2 Gem
sh-ANG #2 Gem/Erlo
p-EGFR (Y1068)
Cleaved Caspase-3
TUNEL
P
mAng1
19636-shRNA v #1 #2
15
mANG
Q
19636-sh-vector
19636-sh-mAng1 #1
19636-sh-mAng1 #2
Absorbance
Cell viability (%)
NS
erlotinib (2 μM)
R
Median (Days)
19636-sh-vector 17.5
19636-sh-vector with Erlo 28.5
19636-sh-vector with Gem/Erlo 25.0
19636-sh-mAng1 #2 26.5
19636-sh-mAng1 #2 with Erlo 25.0
19636-sh-mAng1 #2 with Gem/Erlo 25.0
Percent survival
Days
S
CFPAC-1-sh-vector
CFPAC-1-sh-ANG #2
Absorbance
NS
Treatment of AG1478 (μM)
T
CFPAC-1-sh-vector
CFPAC-1-sh-ANG #2
Absorbance
NS
Treatment of gefitinib (μM)

Figure S7. Knockdown of ANG decreases sensitivity to erlotinib treatment in pancreatic cancer cells. Related to Figure 7.

(A) Cell counting, measured by a Coulter® Particle Counter (Beckman Coulter), of HPAC-1 stable transfectants at the indicated time points. **p < 0.01, ***p < 0.001, Student's *t*-test. Error bars represent SD.

(B) Top, representative images of wound healing assay of HPAC-1 stable transfectants at the indicated time points. Bar, 500 μm. The distance of the wound gaps was determined by using the ImageJ and normalized against the width at time 0, which was plotted diagrammatically in the bottom. **p < 0.01, Student's *t*-test. Error bars represent SD.

(C) Quantification of MTT viability assay of HPAC-1 stable transfectants. The percentage of cell viability in HPAC-1 stable transfectant of the reconstitution of ANG (Flag-ANG) restored expression was normalized against that of vector restored. **p < 0.01, ***p < 0.001, Student's *t*-test. Error bars represent SD.

(D) Left, representative images of colony formation capability of HPAC-1 stable transfectants (HPAC-1-sh-ANG #2) of the reconstitution of ANG (Flag-ANG) restored expression in 6-well plates at day 10. Right, quantification of colony formation capability. Each sample was performed in duplicate for three times. ***p < 0.001, Student's *t*-test. Error bars represent SD.

(E) IB of the reconstitution of ANG (Flag-ANG) restored expression in two independent sh-ANG stable clones of CFPAC-1 cells.

(F) Tumor weight analysis of the indicated groups in (E). n = 5. *p < 0.05, Student's *t*-test.

(G and H) Cell viability assay of HPAC-1 and CFPAC-1 (G) and PTAC-53 and PTAC-50 (H) cells incubated with ANG neutralization Ab compared with those against Flag or Myc Ab. Absorbance was measured at 595 nm with a reference wavelength of 650 nm. **p < 0.01,

Student's *t*-test. Error bars represent SD.

(I) Tumor volume analysis of mice subcutaneously injected with CFPAC-1 cells, followed by treatment with mouse IgG (mIgG) or ANG Ab. Error bars represent SD. n = 8. **p < 0.01, ANOVA analysis.

(J) Immunohistochemistry staining from tumors as indicated in Figure 7E (HPAC-1), stained with the indicated antibodies. Bar, 50 μm.

(K) Left, representative images of colony formation capability of HPAC-1 stable transfectants treated with erlotinib (2 μM) in 6-well plates at day 10. Right, quantification of colony formation capability. Each sample was performed in duplicate for three times. The number of colonies was normalized against that without erlotinib treatment (0 μM). *p < 0.05, Student's *t*-test. Error bars represent SD.

(L) Left, cell viability assay of HPAC-1 stable transfectants. Absorbance was measured at 595 nm with a reference wavelength of 650 nm. Right, quantification of MTT viability assay of HPAC-1 stable transfectants treated with or without erlotinib (2 μM) for 72 hr. The percentage of cell viability in HPAC-1 stable transfectant with erlotinib treatment was normalized against that without erlotinib treatment. *p < 0.05, ***p < 0.001, NS, not significant, Student's *t*-test. Error bars represent SD.

(M) Tumor weight analysis of mice subcutaneously injected with the indicated HPAC-1 cells, followed by treatment with gemcitabine plus either erlotinib (Gem/Erlo) or a matched vehicle (Gem). Error bars represent SD. n = 5. *p < 0.05, Student's *t*-test. NS, not significant.

(N and O) Immunohistochemistry staining from tumors of HPAC-1 (N) and CFPAC-1 (O) stained with the indicated antibodies and a TUNEL kit. Bar, 50 μm.

(P) IB of secreted proteins in mouse 19636 stable transfectants knocking down mAng1 (19636-sh-mAng1 #1 and 19636-sh-mAng1 #2) and empty vector (19636-sh-vector).

(Q) Left, cell viability assay of 19636 stable transfectants. Absorbance was measured at 595 nm with a reference wavelength of 650 nm. Right, quantification of MTT viability assay of 19636 stable transfectants treated with or without erlotinib (2 μM) for 72 hr. The percentage of cell viability in 19636 stable transfectant with erlotinib treatment was normalized against that without erlotinib treatment. ***$p < 0.001$, NS, not significant, Student's *t*-test. Error bars represent SD.

(R) Survival analysis of the indicated groups in mice subcutaneously injected with the indicated 19636 stable transfectants, followed by treatment as indicated.

(S and T) Cell viability assay of CFPAC-1 stable transfectants treated with increasing concentrations of AG1478 (S) and gefitinib (T). Absorbance was measured at 595 nm with a reference wavelength of 650 nm. *$p < 0.05$, ***$p < 0.001$, NS, not significant, Student's *t*-test. Error bars represent SD.

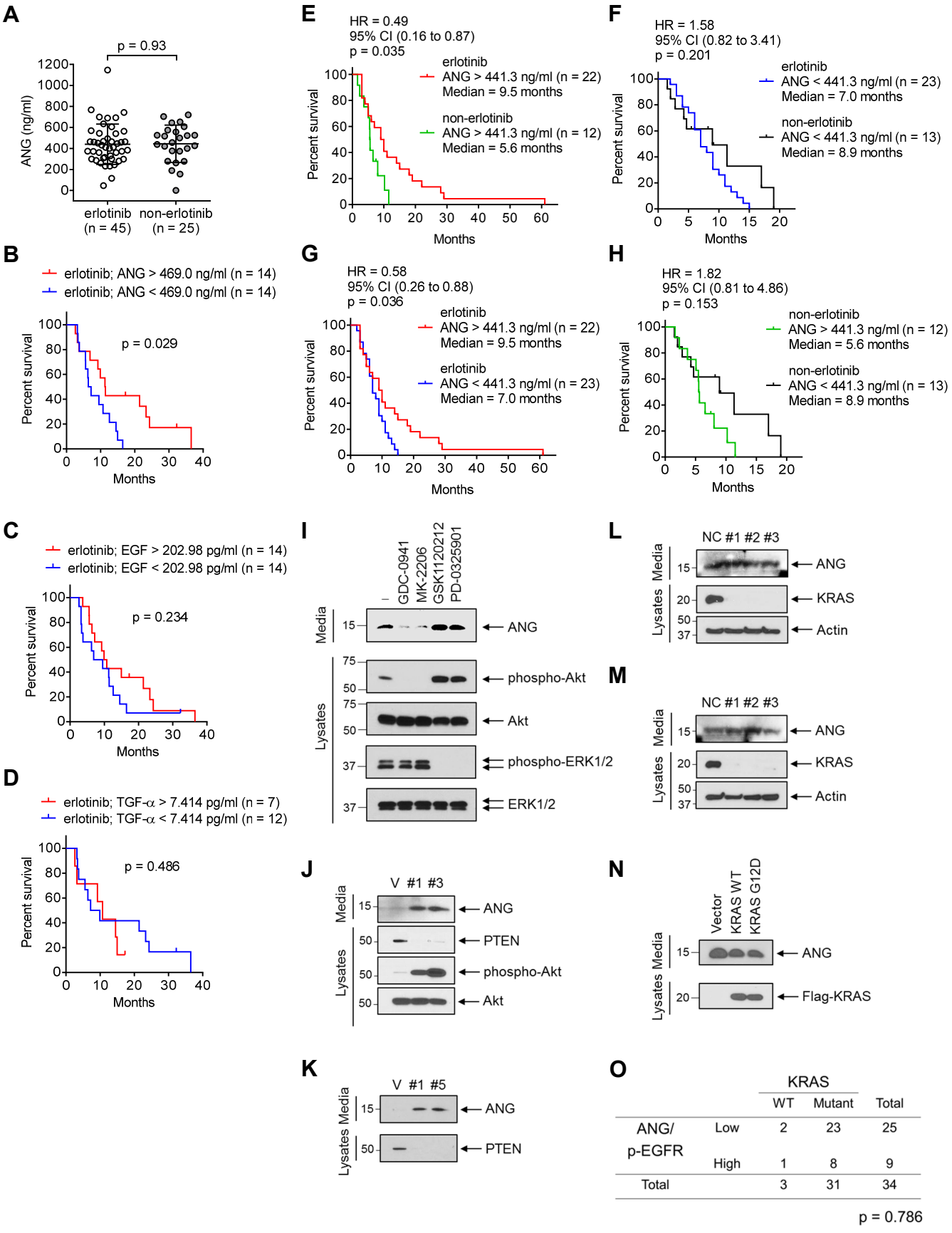
A
p = 0.93
ANG (ng/ml)
erlotinib (n = 45)
non-erlotinib (n = 25)
B
erlotinib; ANG > 469.0 ng/ml (n = 14)
erlotinib; ANG < 469.0 ng/ml (n = 14)
p = 0.029
Percent survival
Months
C
erlotinib; EGF > 202.98 pg/ml (n = 14)
erlotinib; EGF < 202.98 pg/ml (n = 14)
p = 0.234
D
erlotinib; TGF-α > 7.414 pg/ml (n = 7)
erlotinib; TGF-α < 7.414 pg/ml (n = 12)
p = 0.486
E
HR = 0.49
95% CI (0.16 to 0.87)
p = 0.035
erlotinib
ANG > 441.3 ng/ml (n = 22)
Median = 9.5 months
non-erlotinib
ANG > 441.3 ng/ml (n = 12)
Median = 5.6 months
F
HR = 1.58
95% CI (0.82 to 3.41)
p = 0.201
erlotinib
ANG < 441.3 ng/ml (n = 23)
Median = 7.0 months
non-erlotinib
ANG < 441.3 ng/ml (n = 13)
Median = 8.9 months
G
HR = 0.58
95% CI (0.26 to 0.88)
p = 0.036
erlotinib
ANG > 441.3 ng/ml (n = 22)
Median = 9.5 months
erlotinib
ANG < 441.3 ng/ml (n = 23)
Median = 7.0 months
H
HR = 1.82
95% CI (0.81 to 4.86)
p = 0.153
non-erlotinib
ANG > 441.3 ng/ml (n = 12)
Median = 5.6 months
non-erlotinib
ANG < 441.3 ng/ml (n = 13)
Median = 8.9 months
I
–
GDC-0941
MK-2206
GSK1120212
PD-0325901
Media
Lysates
ANG
phospho-Akt
Akt
phospho-ERK1/2
ERK1/2
J
V #1 #3
ANG
PTEN
phospho-Akt
Akt
K
V #1 #5
ANG
PTEN
L
NC #1 #2 #3
ANG
KRAS
Actin
M
NC #1 #2 #3
ANG
KRAS
Actin
N
Vector
KRAS WT
KRAS G12D
ANG
Flag-KRAS
O
KRAS
WT
Mutant
Total
ANG/ p-EGFR
Low
2
23
25
High
1
8
9
Total
3
31
34
p = 0.786

Figure S8. ANG, but not EGF and TGF-α, enhances sensitivity to erlotinib treatment in pancreatic cancer and ANG expression is critically driven via the PTEN/PI3K/Akt activating pathway. Related to Figure 8.

(A) ELISA of ANG in plasma samples of the indicated groups in Figure 8B.

(B–D) Log-rank (Mantel-Cox) test for overall survival of pancreatic cancer patients who received erlotinib therapy (n = 28) in the indicated groups with different levels of ANG (B), EGF (C), and TGF-α (D). The median value (469.0 ng/ml) was used as cutoff to divide patients into high- or low- ANG group based on their ANG concentrations. Cohort size for each group is indicated.

(E and F) Log-rank (Mantel-Cox) test for overall survival of pancreatic cancer patients harboring higher levels of ANG with or without erlotinib therapy (E); lower levels of ANG with or without erlotinib therapy (F). The mean value (441.3 ng/ml) was used as cutoff to divide patients into high- or low- ANG group based on their ANG concentrations. HR (95% CI), Log-rank analysis.

(G and H) Log-rank (Mantel-Cox) test for overall survival of pancreatic cancer patients who received therapy with (G) or without (H) erlotinib in the indicated groups with different levels of ANG. Cohort size for each group is indicated. The mean value (441.3 ng/ml) was used as cutoff to divide patients into high- or low- ANG group based on their ANG concentrations. HR (95% CI), Log-rank analysis.

(I) IB of lysates and secreted proteins from CM in CFPAC-1 cells pretreated with the indicated inhibitors at 37 °C for 24 hr.

(J and K) IB of lysates and secreted proteins from CM in PTEN-deficient Panc-1 (J) and HeLa (K) stable transfectants expressing shRNA targeting PTEN.

(L and M) IB of lysates and secreted proteins from CM in HPAC-1 (L) and CFPAC-1 (M) cells

transfected with individual siRNAs against KRAS.

(N) IB of lysates and secreted proteins from CM in HeLa stable transfectants ectopically expressing KRAS WT and KRAS G12D.

(O) Quantification for the correlation between ANG/p-EGFR expression and KRAS status in pancreatic cancer patients. Fisher's exact test.